FREQUENCY COMPARISON (H_MASER 1400816) - (BNM-SYRTE-FO2)
From MJD 53304 to MJD 53329

The primary frequency standard BNM-SYRTE-FO2 was compared to the hydrogen Maser (1400816) of the laboratory, from MJD 53304 to MJD 53329.

The mean frequency differences measured between the hydrogen Maser 1400816 and fountain FO2 during this period is given in table 1. Additionally, the mean frequency between hydrogen Masers 1400816 and 1400805 are evaluated due to the failure of Maser 1400816 occurred after MJD 53332, in order to compare frequency between Maser 1400805 and FO2 fountain during this period of time 53304 to 53329.

Period (MJD)	**y(HMaser$_{1400816}$ - FO2)** (1)	u_B (2)	u_A (3)	$u_{link\ /\ maser}$ (4)
53304 – 53329	**+ 3283,5**	**6,7**	**2,05**	**1,47**
53304 – 53329	**y(HMaser$_{1400816}$ – Hmaser$_{1400805}$)** **- 4154,86** (8)	**0,03**	**0,02**	

Table 1: Results of the comparison in 1 x 10^{-16} unit.

Figure 1 collects the measurements of fractional frequency differences during the 26th October to 20th November period with their respective statistical uncertainties. The measurements are corrected for the systematic frequency shifts listed below.

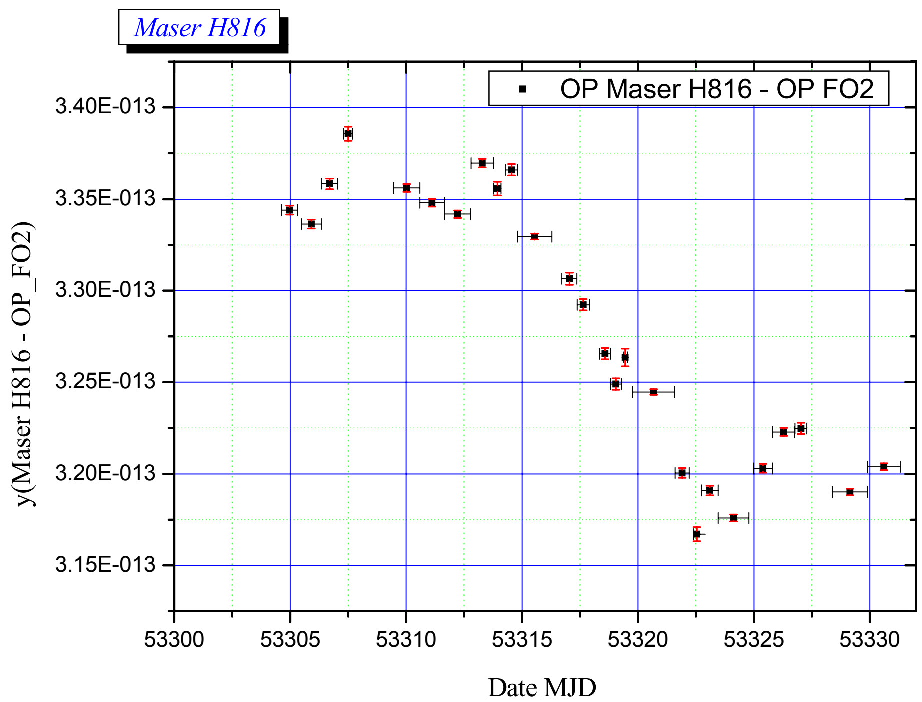

Figure 1: fractional frequency differences between H_Maser1400816 & FO2 from MJD 53304 to MJD 53329

Table of measurements is given bellow (table 2).

SYRTE 61, avenue de l'Observatoire 75014 Paris - France tél 33 (0)1 40 51 22 04 fax 33 (0)1 40 51 22 91 e-mail direction.syrte@obspm.fr
Unité de recherche du CNRS 8630 site syrte.obspm.fr

Start UTC dates unit MJD	Start Local dates unit H:M	Duration H :M	Mean fractional frequency difference $y_{Maser} - y_{FO2}$	type A uncertainties σ_{Stat}	$\sigma_{Collision}$
53304,63414	26/10/2004 17:13	16:42	3,34394E-13	2,48E-16	3,14E-16
53305,50006	27/10/2004 14:00	20:20	3,33635E-13	2,5E-16	3,19E-16
53306,35138	28/10/2004 10:25	16:40	3,35829E-13	2,86E-16	3,54E-16
53307,30189	29/10/2004 09:14	09:35	3,38564E-13	3,89E-16	4,89E-16
53309,4573	31/10/2004 11:58	27:11	3,35602E-13	2,08E-16	2,64E-16
53310,59684	01/11/2004 15:19	25:15	3,34796E-13	2,11E-16	2,66E-16
53311,65791	02/11/2004 16:47	27:11	3,34175E-13	1,96E-16	2,43E-16
53312,79576	03/11/2004 20:05	23:36	3,36963E-13	2,23E-16	2,78E-16
53313,78125	04/11/2004 19:45	07:43	3,35572E-13	3,68E-16	2,91E-16
53314,30455	05/11/2004 08:18	11:52	3,36596E-13	3,09E-16	2,91E-16
53314,80132	05/11/2004 20:13	35:37	3,3295E-13	1,66E-16	2,06E-16
53316,71729	07/11/2004 18:12	15:40	3,30652E-13	3,3E-16	4,2E-16
53317,3748	08/11/2004 09:59	12:39	3,29225E-13	3,07E-16	3,75E-16
53318,34519	09/11/2004 09:17	11:15	3,26559E-13	3,13E-16	3,86E-16
53318,81854	09/11/2004 20:38	11:02	3,24902E-13	3,16E-16	3,28E-16
53319,35903	10/11/2004 09:37	04:33	3,26351E-13	4,85E-16	3,28E-16
53319,76782	10/11/2004 19:25	43:26	3,24466E-13	1,57E-16	1,97E-16
53321,59669	12/11/2004 15:19	14:45	3,20037E-13	2,65E-16	3,3E-16
53322,38854	13/11/2004 10:19	06:54	3,16706E-13	3,83E-16	4,99E-16
53322,74519	13/11/2004 18:53	17:06	3,19087E-13	2,53E-16	3,17E-16
53323,46545	14/11/2004 12:10	31:48	3,1759E-13	1,82E-16	2,3E-16
53324,9766	16/11/2004 00:26	19:47	3,20298E-13	2,36E-16	2,9E-16
53325,80439	16/11/2004 20:18	22:59	3,22282E-13	2,16E-16	2,67E-16
53326,7735	17/11/2004 19:33	12:23	3,22477E-13	3,07E-16	3,83E-16
53328,39141	19/11/2004 10:23	36:11	3,19001E-13	1,74E-16	2,22E-16

Table 2: Measurements H_Maser1400816 - FO2 from MJD 53304 to 53329

Start UTC dates unit MJD	Stop UTC dates unit MJD	Duration & Measurement Rate	Mean frequency difference normalized $y_{Maser} - y_{FO2}$ **(1)**	type A uncertainty σ_{Stat} & $\sigma_{Collision}$	Uncertainty due to the dead times $\sigma_{deadTime}$ **(4)**
53304,63414	53329,89905	Total duration : 25,26491 d Total measurements 20,0805 d Measurement Rate : 79,48 %	Standard Mean $\bar{y}$ = **3283,5** x **10^-16** Weighted Mean **(5)**: $\bar{y}$ = **3279,8 x 10^-16** Linear fit regression **(6)**: $\bar{y}$ = **3285,7 x 10^-16** High order polynomial fit **(6)**: $\bar{y}$ = **3283,5 x 10^-16** Mean from Phase differences **(7)**: $\bar{y}$ = **3284,4 x 10^-16**	σ_A = 0,**76** x **10^-16** **(3)** Linear fit regression**(6)** σ_y = 0,**763** x **10^-16** High order Polynomial fit **(6)** σ_y = 1,**9** x **10^-16** From Phase differences σ_A = 0,**611** x **10^-16**	$\sigma_{deadTime}$ = **1,08 10^-16**

Table 3: Statistics of measurements

(1) Fractional frequency difference obtained after systematic relative frequency shifts correction:

$$y_{Maser-FOM} = \frac{\delta(\nu)_{Zeeman2}}{\nu_0} + \frac{\delta(\nu)_{BlackBody}}{\nu_0} + \frac{\delta(\nu)_{Collision+CavityPulling}}{\nu_0} + \frac{\delta(\nu)_{redshift}}{\nu_0} - \frac{f_{mesure}}{\nu_0}$$

with $\nu_0 := 0.9192631770\ 10^{10}$. The fractional mean frequency is calculated by four ways as mentioned in table 3 in order to have comparison between statistical computation such as standard mean, weighted mean, with a linear fit and with phase differences.

(2) Systematic uncertainty $\sigma_B = u_B$ in witch statistical effect of cold collisions and cavity pulling is removed (see **Annexe 1**)

$$\sigma_B = \left(\sigma_{Zeeman2}^2 + \sigma_{BlackBody}^2 + \sigma_{Collision_{Syst}}^2 + \sigma_{Microwave\_Spectrum}^2 + \sigma_{Microwave\_Leakage}^2 + \sigma_{Ramsey\_Rabi}^2 + \sigma_{Recoil}^2 + \sigma_{second\_Doppler}^2 + \sigma_{Background\_collsions}^2 + \sigma_{Redshift}^2\right)^{(1/2)}$$

(3) Statistical uncertainty $\sigma_A = u_A$, in which is taken into account the statistical uncertainty on each measurement σ_{Stat_i} and statistical effect on the cold collisions and Cavity Pulling measurement $\sigma_{Collision_i}$ (see **Annexe 4** Linear Regression on the frequency measurements & **Annexe 5**) : $\sigma_A = \sqrt{\dfrac{1}{\displaystyle\sum_{i=1}^{n} \frac{1}{\sigma_{Stat_i}^2 + \sigma_{Collision_i}^2}}}$

(4) Uncertainty due to the link between H_Maser and the fountain FO2 $u_{link\_Maser} = \sqrt{\sigma_{link\_Lab}^2 + \sigma_{dead\_time}^2}$ where $\sigma_{link\_Lab} = 0.1\ 10^{-15}$ and σ_{dead_time} is the uncertainty due to the dead times during measurements (see **Annexe 3**)

(5) Weighted Mean by statistical uncertainty on each measurement

$$y_j := \frac{\displaystyle\sum_{i=1}^{n_j} \frac{y_i}{\sigma_{Ai}^2}}{\displaystyle\sum_{i=1}^{n_j} \frac{1}{\sigma_{Ai}^2}}$$

where

$$\sigma_{A_i} = \frac{1}{\sqrt{\dfrac{1}{\sigma_{Stat_i}^2 + \sigma_{Col_i}^2}}}$$

(6) Mean frequency obtained by a linear fit by weighted least squares with statistical uncertainty on each measurement and by an high order polynomial fit (see **Annexe 4**).

(7) Mean frequency obtained by phase differences that is the retained result (see **Annexe 5**).

(8) Mean frequency obtained by phase differences between Masers 1400805 and 1400816 (see **Annexe 6**).

ANNEXE 1

Uncertainties of systematic effects in the FO2 fountain

Systematic effects taken into account are the quadratic Zeeman, the Black Body, the cold collision and cavity pulling corresponding to the systematic part (see annexe 2), the microwave spectral purity and the microwave leakage, the Ramsey Rabi pulling, the recoil, the 2^{nd} Doppler and the background collisions. Each of these effects is affected by an uncertainty. The uncertainty of the red shift effect is also included in the systematic uncertainty budget and gives

$$\sigma_B = \left(\sigma_{Zeeman2}{}^2 + \sigma_{BlackBody}{}^2 + \sigma_{Collision_{Syst}}{}^2 + \sigma_{Microwave\_Spectrum\_Leakage}{}^2 + \sigma_{first\_Doppler}{}^2 + \sigma_{Ramsey\_Rabi}{}^2 + \sigma_{Recoil}{}^2 + \sigma_{second\_Doppler}{}^2 + \sigma_{Background\_collisions}{}^2 + \sigma_{Redshift}{}^2 \right)^{(1/2)}$$

Here are mentioned the uncertainties of the different effects (see **Annexe 2** and **[ref, 1]**):

Quadratic Zeeman effect	:	$\sigma_{Zeeman2} := 0.35\ 10^{-16}$	(continuously measured)
Black Body effect	:	$\sigma_{BlackBody} := 0.25\ 10^{-15}$	(calculated)
Systematic Collisional effect	:	$\sigma_{Collision_{Syst}} := 0.7070\ 10^{-16}$	(continuously measured)
Microwave Spectrum purity & Leakage effect	:	$\sigma_{Microwave\_Spectrum\_Leakage} := 0.45\ 10^{-15}$	(measured)
First order Doppler effect	:	$\sigma_{first\_Doppler} := 0.38\ 10^{-15}$	(calculated and measured)
Rabi-Ramsey effect	:	$\sigma_{Ramsey\_Rabi} < 0.10\ 10^{-15}$	(calculated)
Recoil effect (see **[ref, 3]**)	:	$\sigma_{Recoil} := 0.10\ 10^{-15}$	(calculated)
Second order Doppler effect	:	$\sigma_{second\_Doppler} := 0.8\ 10^{-17}$	(calculated)
Background effect	:	$\sigma_{Background\_collisions} := 0.10\ 10^{-15}$	(evaluated)
Red shift effect	:	$\sigma_{Redshift} := 0.2\ 10^{-16}$	(calculated)

For the whole July period it gives

$$=> \quad \boxed{\sigma_B = 0.670\ 10^{-15}}$$

ANNEXE 2

1 - Measurement of the collisional frequency shift and the cavity pulling

Collisional shift takes into account the effect of the collisions between cold Caesium atoms and the effect of "Cavity Pulling" whose influence also depends on the number of atom. This effect is measured in a differential way during each integration and its determination thus depends on the duration of the measurement and on the stability of the clock, thus the uncertainty on the determination of the collisional shift is mainly of statistical nature. To the statistical uncertainty we add a type B uncertainty of 1% of frequency shift resulting from the imperfection of the adiabatic passage method (see the article **[ref. 4]**).

Figure 2 visualizes the relative frequency shift due to the effect of the collisions and "Cavity Pulling" of the atomic fountain FO2 taken in low density, between the MJD 53304 and 53329 with the statistical uncertainty of each measurement, $\sigma_{Collision(i)}$.

Figure 3 shows the Allan deviation of a differential measurement using high and half atom density fountain configurations during MJD 53202 (from MJD 53202,72361 to MJD 53206,00278), in order to correct of the cold collisional shift for this period. FO2 was operated alternatively (every 50 clock cycles) at low atomic density (red circle) and high density (black square) against the cryogenic oscillator weakly phase locked on the H_Maser. The measured density ratio between low and high densities is **0,50001666±0,000033**. The frequency difference between both densities is used to determine the collisional coefficient which is used to correct each data point. The blue triangle points represent the Allan deviation of the frequency difference between low and high densities when the points are corrected. The Allan deviation varies as $\tau^{-1/2}$and reaches 10^{-16} after 100000s.

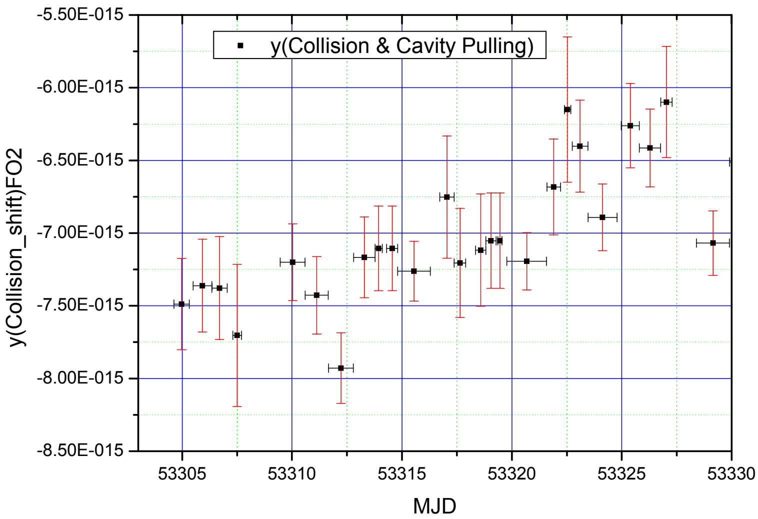

Figure 2: Fractional frequency shift due to cold collisions and Cavity Pulling from MJD 53304 to MJD 53329

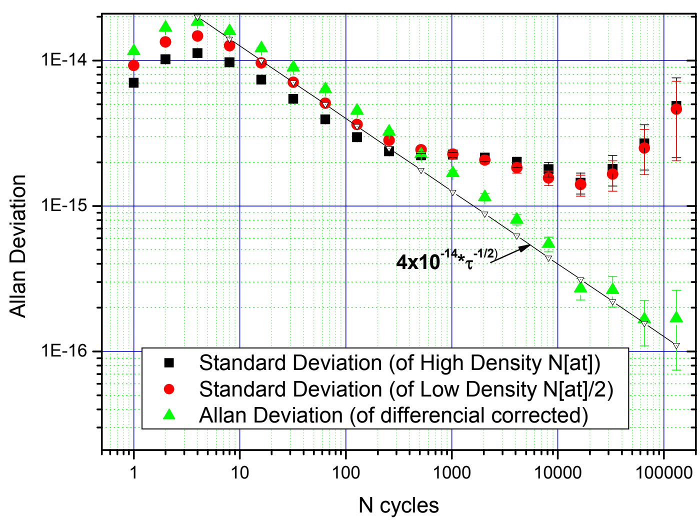

Figure 3: Allan deviation of measurements of the shift frequency in high and low atom density and their differences during MJD 53309,5 to MJD 53324,83333

The weighted mean $y_{Collision_{moy}} = \dfrac{\sum_{i=1}^{n} \dfrac{y_{Collision_i}}{\sigma_{Collision_i}^2}}{\sum_{i=1}^{n} \dfrac{1}{\sigma_{Collision_i}^2}}$ of collisionnal shift gives for November is $y_{Collision_{moy}} := -0.7070\ 10^{-14}$

The systematic effect of these shifts is evaluated by the 1% part of the mean frequency collisional shift during July:

$$\sigma_{Collision_{Syst}} = \frac{1}{100}\left|y_{Collision_{moy}}\right| = \sigma_{Collision_{Syst}} := 0.7070\ 10^{-16}$$

This value is taking into account in the systematic uncertainty evaluation σ_B (see annexe 1).

2 - Measurement of the 2nd order Zeeman frequency shift

Every 15 min the frequency of the central fringe of the field linearly dependant transition $|F=3, m_F=1\rangle \longrightarrow |F=4, m_F=1\rangle$ is measured. This frequency is directly proportional to the field as $\delta(\nu_{11})=K_{Z1}B$ with K_{Z1} = 7,0084 Hz.nT^{-1} (see **[ref. 5]** vol. 1 p37 table 1.1.7(a)). In the fountain, the transition $|F=3, m_F=0\rangle \longrightarrow |F=4, m_F=0\rangle$ is shifted by quadratic Zeeman effect and depend on squared magnetic field as $\delta(\nu_{00})=K_{Z2}B^2$ with K_{Z2} = 42,745 mHz.µT^{-2} (see **[ref. 5]** vol. 1 p37 table 1.1.7(a)). Knowing K_{Z1} and measuring δ(ν11) allow good estimation of Zeeman quadratic shift as $\delta(\nu_{00}) = K_{Z2}\left(\dfrac{\delta(\nu_{11})}{K_{Z1}}\right)^2$. The relative quadratic Zeeman frequency shift is calculated by $\dfrac{\delta(\nu_{00})}{\nu_0} = 427{,}45\times10^{-6}\left(\dfrac{\delta(\nu_{11})}{700{,}84}\right)^2$ with $\delta(\nu_{11})$ in Hz unit and ν_0 = 9192631770 Hz. And the uncertainty is evaluated by $\dfrac{\Delta(\delta(\nu_{00}))}{\nu_0} = 427{,}45\times10^{-6}\times\dfrac{2\times\overline{B}\times\Delta(B)}{\nu_0}$ with B in mG. Figure 4 displays the tracking of the central fringe during MJD 53305 to MJD 53331. This shows the good stability of the magnetic field in the interrogation zone. The frequency variation is taken as in an interval of standard deviation ±0,131Hz. When taking the standard deviation of variation of the magnetic field $\Delta(B)$ over the whole measurement period as the field uncertainty, we find 18,7 pT. The corresponding uncertainty of the correction of the second order Zeeman effect is 0,35x10^{-16},

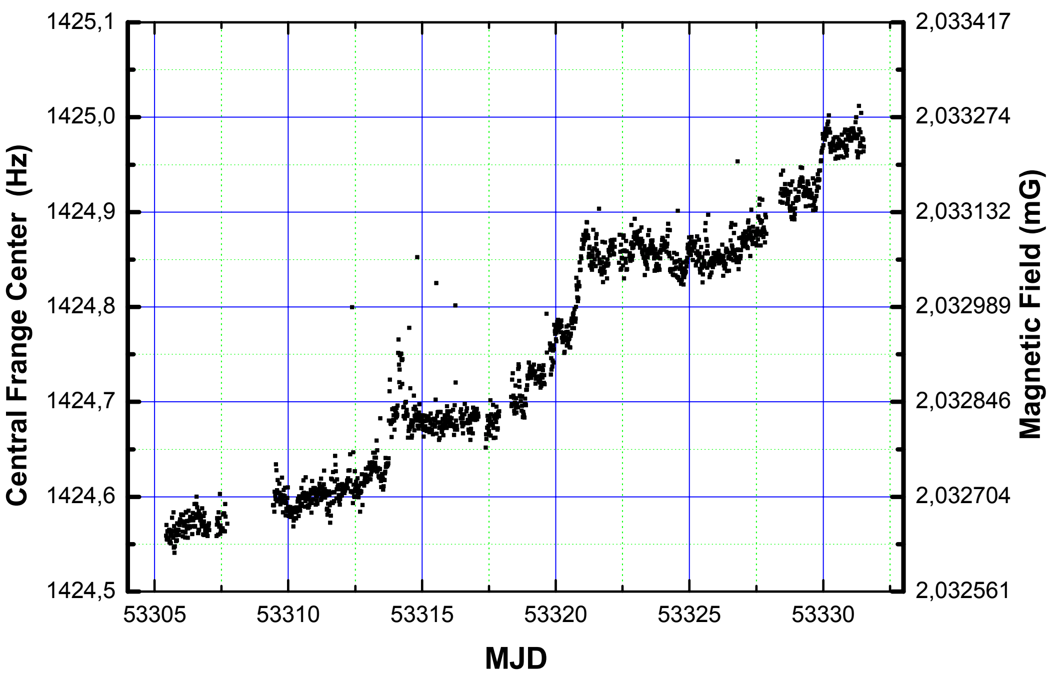

Figure 4: tracking of the central fringe from MJD 53305,43791 to MJD 53331,53059

3 - Measurement of the Blackbody Radiation shift

An ensemble of 3 platinum thermistors monitors the temperature and its gradient inside the vacuum chamber. The average temperature is ~25,5°C with a gradient smaller than 1 K along the atom trajectory. The correction is

$$\left(\frac{\delta(\nu)}{\nu_0}\right)_{Blackbody} = -\frac{0.0001573\left(\frac{T}{300}+0.9105000000\right)^4}{\nu_0} = -0.168281\ 10^{-13} \pm 0.25\ 10^{-15}$$

4 - Effect of the Microwave Spectrum effect and leakage effect

The clock frequency is measured as a function of the microwave power. Every 50 cycles the atom interrogation is alternated between 4 configurations of π/2, low density and high density, and 3π/2, low density and high density. It allows extrapolating and removing the variation of the collision shift in the comparison between π/2 and 3π/2 pulses. We find

$$\frac{\delta(\nu)_{Microwave\_Spectrum\_Leakage}}{\nu_0} = -0.44\ 10^{-15} \pm 0.45\ 10^{-15}$$

5 - Measurement of the residual 1st order Doppler effect

We determined the frequency shifts caused by asymmetry of the coupling coefficients of the two microwave feedthroughs and the error on the launching direction by coupling the interrogation signal either "from the right" or "from the left" or symmetrically into the cavity. The measured shift is

$$\left(\frac{\delta(\nu)}{\nu_0}\right)_{first\_Doppler} = 0.45\ 10^{-14} \pm 0.38\ 10^{-15}$$

In FO2 fountain we feed the cavity symmetrically at 1% level both in phase and in amplitude. This shift is thus reduced by a factor of 100 and became negligible. The quadratic dependence of the phase becomes dominant. A worse case estimate based on **[ref. 6]** gives fractional frequency shift of 3 x 10^{-16} which we take as uncertainty due to the residual 1st order Doppler effect.

6 – Rabi and Ramsey effect and Majorana transitions effect

An imbalance between the residual populations and coherences of $m_F < 0$ and $m_F > 0$ states can lead to a shift of the clock frequency estimated to few 10^{-18} for a population imbalance of 10^{-3} that we observe in FO2 (see **[ref. 7]** and **[ref. 8]**).

7 – Microwave recoil effect

The shift due to the microwave photon recoil was investigated in **[ref. 3]**. It is smaller than 1,4 x 10^{-16} .

8 – Gravitational red-shift and 2nd order Doppler shift

The relativistic effect is evaluated as: $\frac{\delta(\nu)_{redshift}}{\nu_0} = 0.625\ 10^{-14}$ with an uncertainty $\sigma_{Redshift} = \pm 0.2\ 10^{-16}$

The 2nd order Doppler shift is less than 0,08 x 10^{-16} .

9 – Background collisions effect

The vacuum pressure inside the fountains is typically a few 10^{-8} Pa. Based on early measurements of pressure shift (see **[ref. 5]**) the frequency shift due to collisions with the background gas is < 10^{-16}.

See **[ref. 9]** for recent evaluations of systematic effects of FO2 fountain.

ANNEXE 3

Uncertainty due to the dead time during the measurements

A statement of the distribution of the missed periods of measurements by FO2 is represented in figure 5,

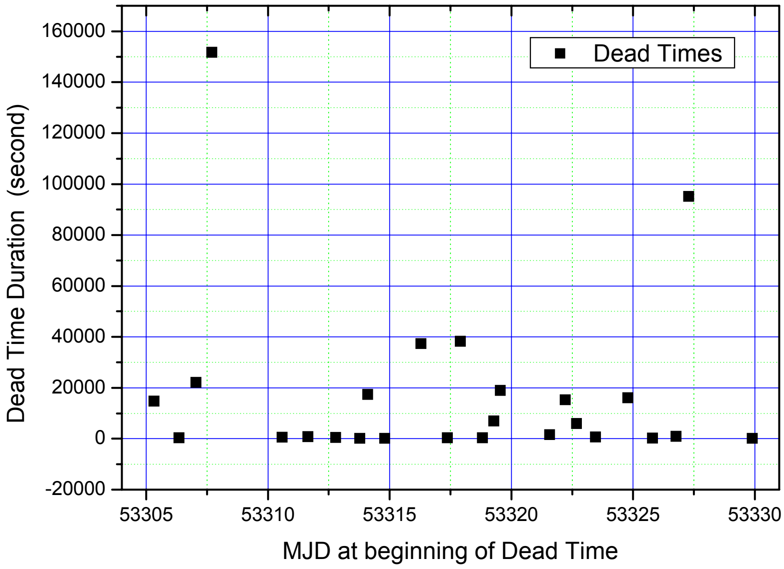

Figure 5: Dead Times on measurements of H_ Maser1400816 –FO2 over the period from MJD 53305 to 532331

For the period of the MJD 53304 until the MJD 53330, the variations of phase between hydrogen Maser 1400805 and the hydrogen Maser 1400816 were sampled every 100s. After removing a linear fit from the phase variations to carry out the calculation of standard deviation in the temporal field, we evaluated the uncertainty associated with the H_Maser according to time (by step of 100s). One obtains the phase variations between H_Maser 1400805 and the H_Maser 1400816. They are plotted on figure 6.

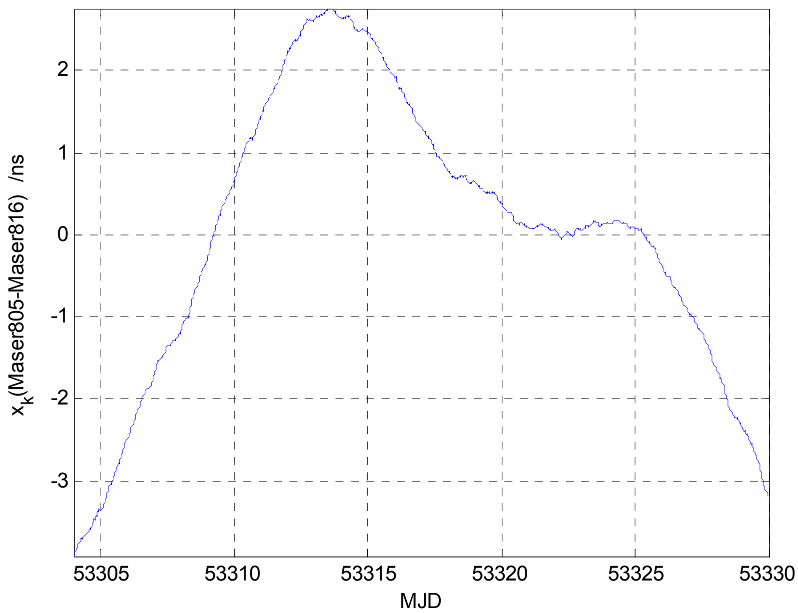

Figure 6: phase data x(Maser805-Maser816) linear drift removed x(H805-H816) MJD 53304 to MJD 53330

Frequency stability analyzes were performed using the overlapping Allan deviation on frequency data and represented for October to November in figure 7 and similarly time stability analyzes with a time deviation were computed and represented for October to November in figure 8 .

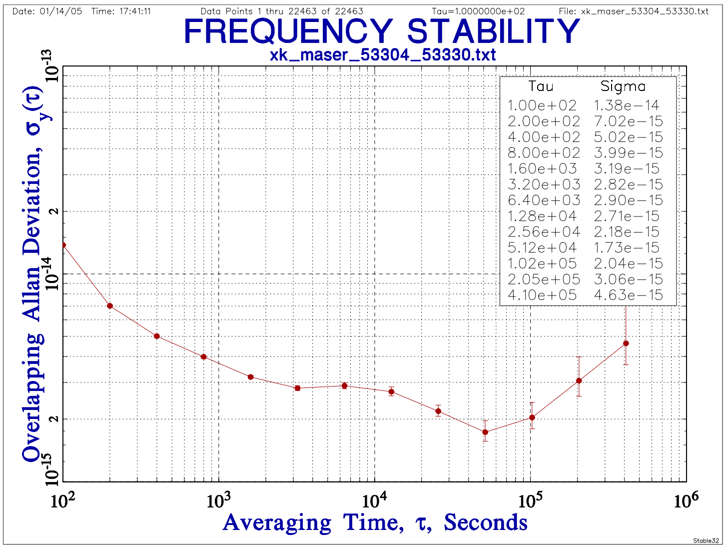

Figure 7: frequency stability analyzes x(HMaser805 - HMaser816) from MJD 53304 to MJD 53329

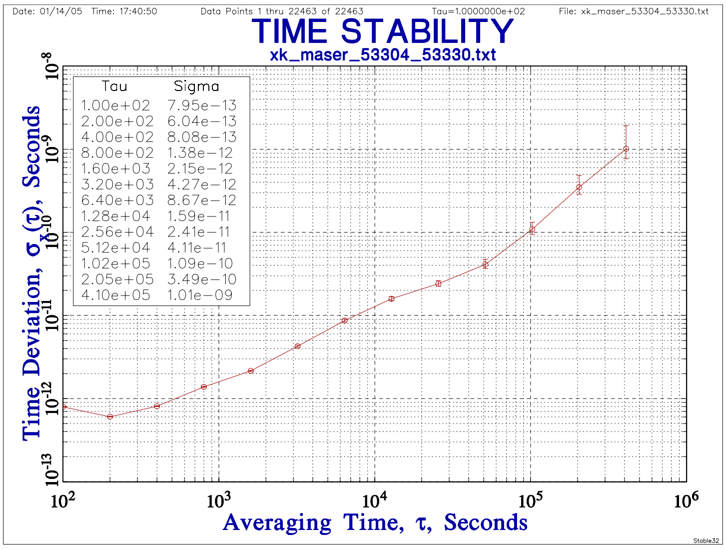

Figure 8: time stability analyzes from x(HMaser805 - HMaser816) from MJD 53304 to MJD 53329

Table 4 provides the standard deviations of the phase fluctuations of the hydrogen Maser 1400805 with respect to the hydrogen Maser 1400816 associated to each dead time according to their duration for the period October to November 2004. The quadratic sum gives

$$\sum_{i=1}^{25} \sigma_{x_i}(\tau)^2 = 0.5826442027\ 10^{-19}$$

The October November 2004 period of FO2 measurements is 25,26491 days or $T := 0.2182888224\ 10^{7}$ seconds. One thus finds the standard deviation of the fluctuations of frequency due to the dead times in measurements by the ratio

$$\sigma_{deadTime} = \frac{\sqrt{\sum_{i=1}^{25} \sigma_{x_i}(\tau)^2}}{T} = \sigma_{deadTime} = 0.1079\ 10^{-15}$$

With taking $\sigma_{link\_Maser} = \sqrt{\sigma_{link\_lab}^{\ 2} + \sigma_{deadTime}^{\ 2}}$ that gives $\boxed{\sigma_{link\_Maser} = 0.1471\ 10^{-15}}$

End Date of each measurement (MJD)	Dead Time Duration second	σ_x
53305,32998	14695	1.7464e-11
53306,34728	354,00002	8.0830e-13
53307,04582	22124,00004	2.2430e-11
53307,70119	151728	2.0433e-10
53310,58994	596	1.1091e-12
53311,64892	776,00003	1.0284e-11
53312,79054	451,00004	9.5812e-13
53313,7791	185,99999	6.0360e-13
53314,10278	17433,00001	1.9484e-11
53314,79899	200,99997	6.0360e-13
53316,28535	37320	3.0114e-11
53317,37007	408,99998	8.0830e-13
53317,90189	38300,99998	3.1143e-11
53318,81394	398	8.0830e-13
53319,27826	6977,99999	9.5520e-12
53319,54861	18939,99997	2.0514e-11
53321,57755	1654,00003	2.2328e-12
53322,21127	15316,00003	1.8184e-11
53322,67604	5973,99999	8.0213e-12
53323,45769	671,00001	1.2472e-12
53324,79045	16083,00002	1.8637e-11
53325,8009	300,99998	6.6522e-13
53326,76203	990,99998	1.6491e-12
53327,28947	95208	9.6626e-11
53329,89905	205	6.0360e-13

Table 4: Statement of the dead times of H_Maser 1400816 - FO2 measurements between MJD 53304 and MJD 53329

ANNEXE 4

Linear Regression on the frequency measurements on period MJD 53304-53329

One calculates the linear regression line by the algorithm of weighted least squares by statistical uncertainty of each frequency differences measurements:

$$y_k = a_1 + a_2\, t$$

Figure 9 gives the representation of frequency measurements and the linear fit resulting from weighted least squares by inverse of squares statistical uncertainty $1/\sigma_{Ai}^{\ 2}$.

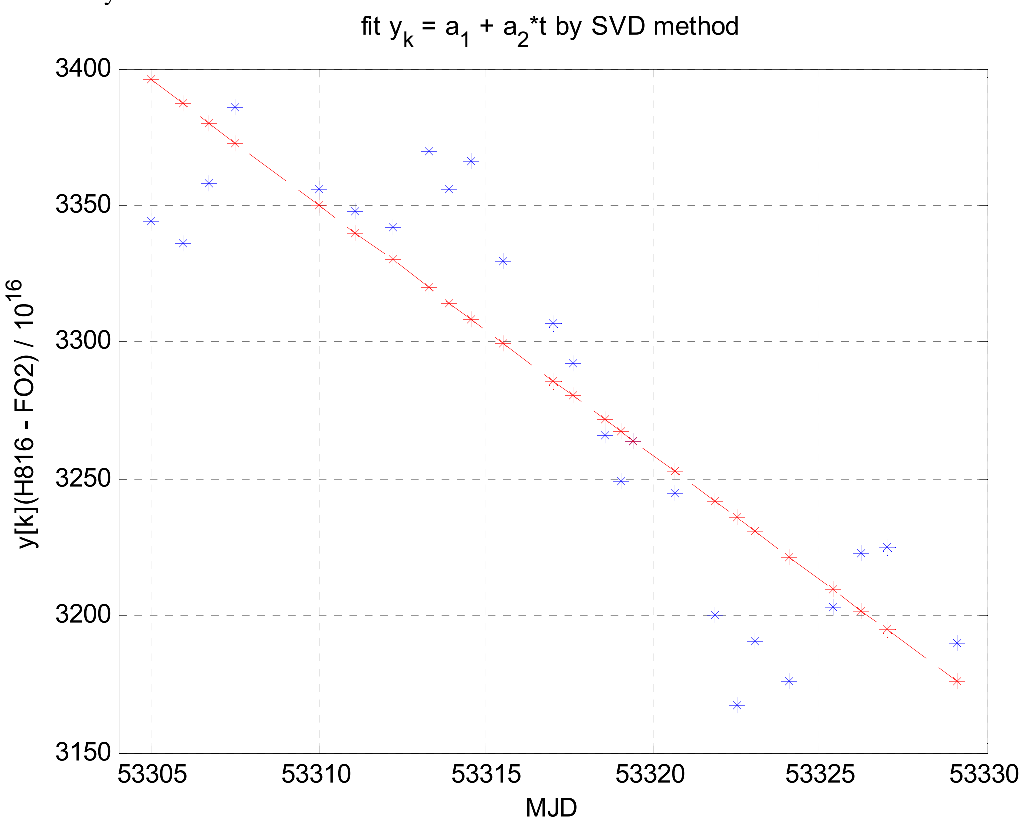

Figure 9: linear regression on the frequency y(HMaser-FO2) between MJD 53304 and 53329 weighted by uncertainty : $1/\sigma_{Ai}^{\ 2}$

Summary of statistical terms:
Coefficient a1 = 4.89224666835326e-011 sigma(a1) des yk de FO2 = 5.85902408664645e-013
Coefficient a2 = -9.11413535682658e-016 sigma(a2) des yk de FO2 = 1.09888895293324e-017

Covariance Matrix:
3.43281632479032e-025 -6.43841678965355e-030
-6.43841678965355e-030 1.20755693087871e-034
Mean date of measurements = 53317.063645
Frequency mean by linear fit y_FO2 = 3.28573194625792e-013
Uncertainty propagation at t_moyen uc_y_FO2 = 7.63055228772718e-017

Degree of Freedom DEF = 23
Mean Square Error = Chi2/DEF = 72.3313659030223
Birge ratio Rb (chi2/DEF)^1/2 = 8.50478488281875
Limit of Birge ratio Rb = 1+sqrt(2/DEF) = 1.29488391230979
Probability of a sample y(Maser-FO2) being superior of Chi2|DEF = 0
SSR Sum Square of Residues = 2.72305810760113e-028
RMS Root Mean Square of Residues = 1.65016911484888e-014
Allan Deviation at T with assumption of White Frequency Noise = 3.24683570069502e-016
T total duration + tau0 = 2270203.75295983 (seconds)
tau0 (mean time between measurements) = 87315.5289599933 (seconds)

High order Polynomial fit on the frequency measurements on period MJD 53304-53329

One calculates the polynomial fit by the algorithm of least squares on each frequency differences measurements:

$$y = \sum_{i=0}^{M} p_{i+1}\, t^{(M-i)}$$

For data measurements collected by interval of 2 hours duration we have the figure 10, 254 points with mean time interval duration of 8651 seconds during MJD 53304-53329 periods. With a polynomial of order M=19 we smooth the maser noise on about 2 days. We obtain the polynomial fit represented on figure 11.

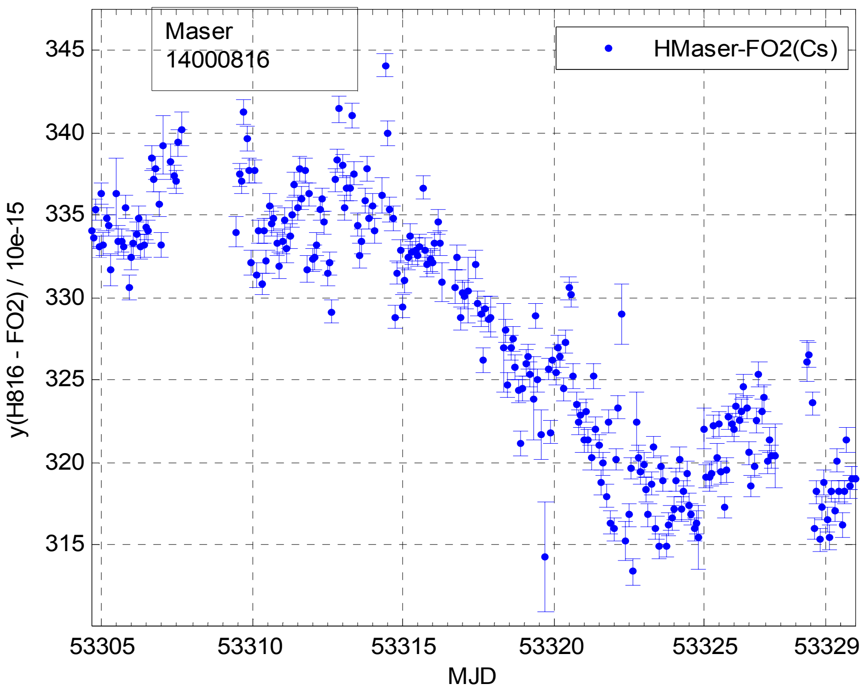

Figure 10: frequency 2H samples y(H816-FO2) MJD 53304 - 53329

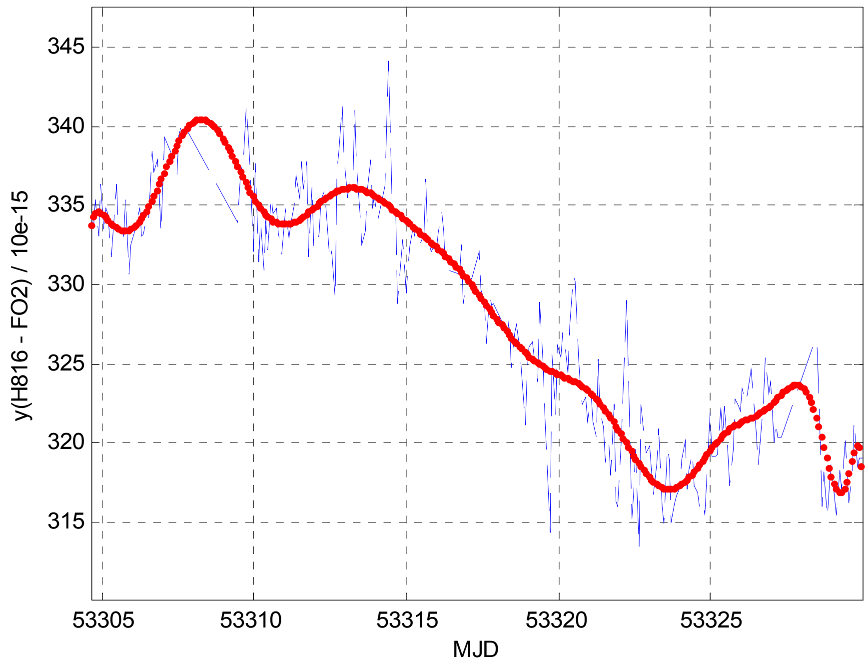

Figure 11: frequency 2H samples y(H816-FO2) and the order 19 polynomial fit MJD 53304 - 53329

By integrating the fit polynomial from 53304 to 53329 we obtain an averaging frequency $\boxed{\mathbf{y_{moy(H816\text{-}FO2)} = 3283{,}51 \times 10^{-16}}}$.

Statistical uncertainty is evaluated by the frequency stability analysis of residuals. Figure 12 shows an overlapping Allan deviation and figure 12-bis shows a law of white noise frequency modulation of 2,8 x $10^{-13}\tau^{-1/2}$. An extrapolated value until 25 days is obtained by this law :

$$\boxed{\boldsymbol{\sigma_y(\tau=25d) = 1{,}9 \times 10^{-16}}}$$

This value is added with the statistical uncertainty σ_A obtained from each measurement

$$\sigma_A = \sqrt{\frac{1}{\displaystyle\sum_{i=1}^{n} \frac{1}{\sigma_{Stat_i}^{\ 2} + \sigma_{Collision_i}^{\ 2}}}}$$

and resulting in σ_A = **0,76** x **10^{-16}** and finally the statistical uncertainty of mean frequency $\mathbf{y_{moy(H816\text{-}FO2)}}$ **= 3283,51 x 10^{-16}** .

$$u_A = \sqrt{\sigma_A^{\ 2} + \sigma_y(\tau = 25\ d)^2}$$

$$u_A := 0.2051\ 10^{-15}$$

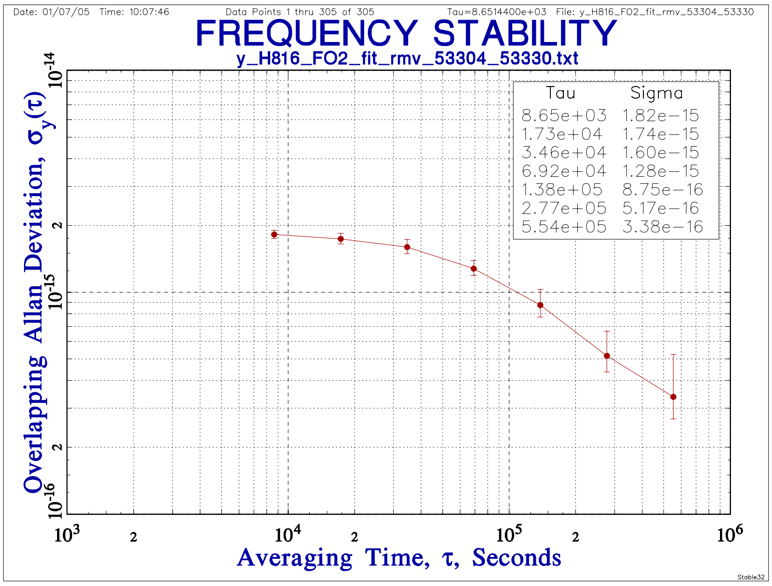

Figure 12: frequency stability analyzes y(HMaser805 – FO2) order 19 polynomial fit removed, from MJD 53304 to MJD 53329

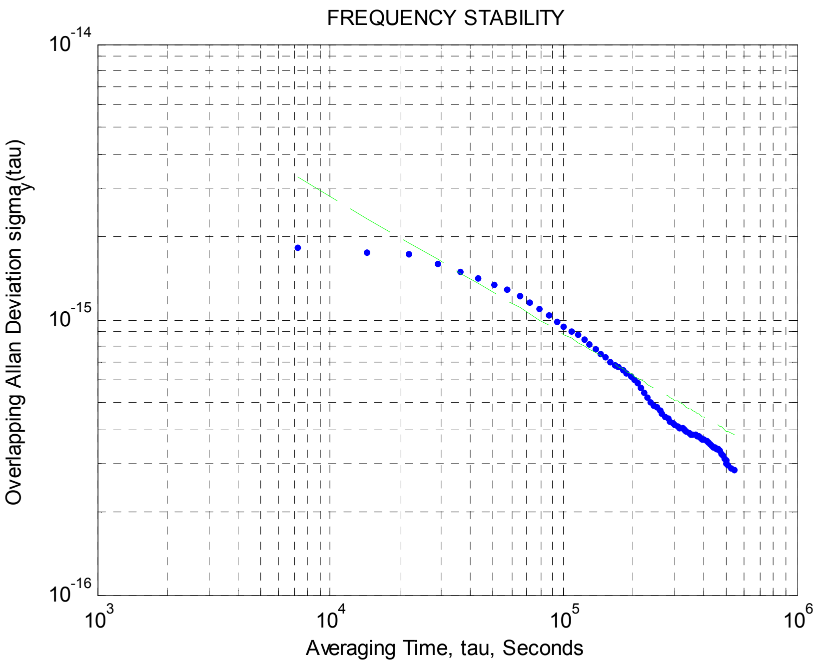

Figure 12-bis: frequency stability analyzes y(HMaser805 – FO2) over all tau from MJD 53304 to MJD 53329

ANNEXE 5

Mean Frequency computed by phase differences

On figure 13 is showed the evolution of the differences in fractional frequency y(t). At each period of integration is evaluated a frequency $\tilde{y}_k$ corresponding to the interval $t_{k+1} - t_k$. The relation binding the variations of phase and the instantaneous frequency deviations is given by

$$y_k = \frac{x_{k+1} - x_k}{t_{k+1} - t_k} \tag{1}$$

$$y(t) = \frac{\nu_{HMaser} - \nu_{FO2}}{\nu_0}$$

$\nu_0 = 9{,}192631770\ \mathrm{GHz}$

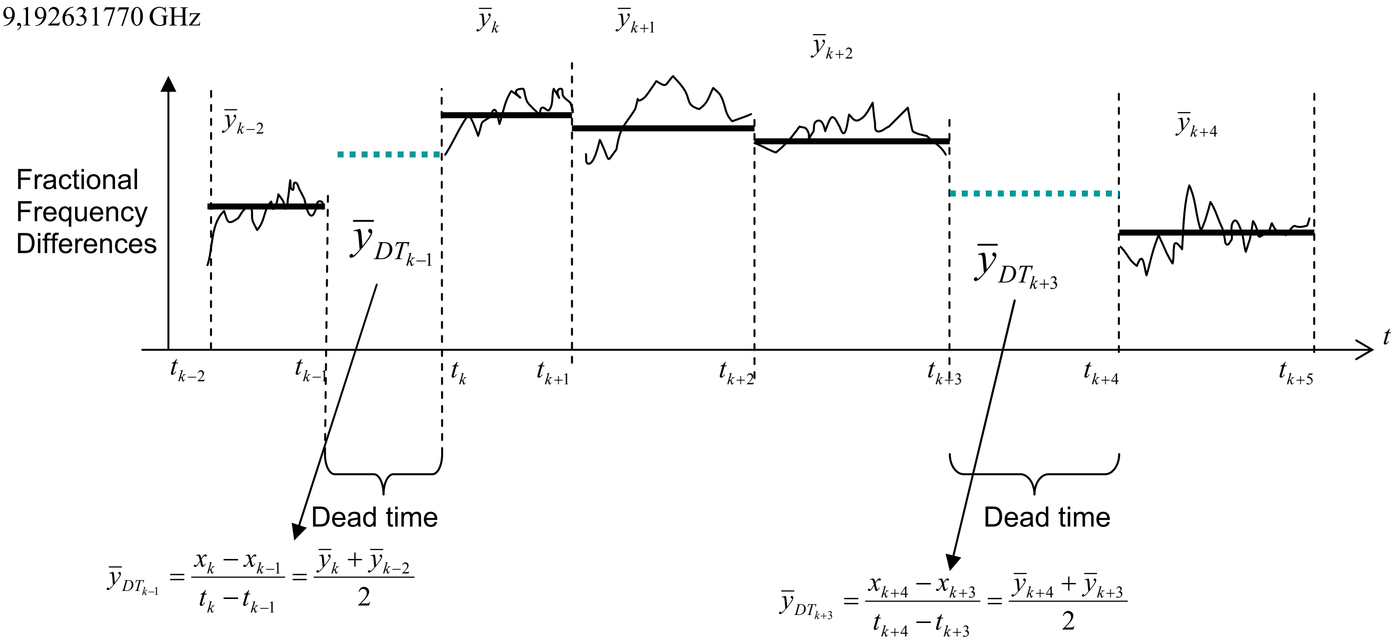

Figure 13: contribution of frequency measurements on the mean frequency calculated

By using equation (1) we have $x_{k+1} - x_k = (t_{k+1} - t_k)\, y_k$

and for addition of consecutive phase differences we find $\sum_{k=1}^{N} (x_{k+1} - x_k) = x_{N+1} - x_1 = \sum_{k=1}^{N} (t_{k+1} - t_k)\, y_k$

During dead time we evaluated the mean frequency by interpolating the mean frequency between two intervals of integrations noted:

$$y_{DT_{m-1}} = \frac{1}{2} y_m + \frac{1}{2} y_{m-1} \tag{2}$$

The contributions of N duty intervals with the frequency measurements y_k and *M* idle intervals with the mean frequency extrapolating between two intervals of integration y_{DT} give the summation

$$\left(\sum_{k=1}^{N} (t_{k+1} - t_k)\, y_k \right) + \left(\sum_{m=1}^{M} (t_{m+1} - t_m)\, y_{DT_m} \right) = x_{fin} - x_{deb} \tag{3}$$

$$\boxed{y_{moy} = \frac{x_{fin} - x_{deb}}{86400\ MJD_{fin} - 86400\ MJD_{deb}}} \tag{4}$$

Where $(x_{fin} - x_{deb})$ represents the phase variation between the whole periods of integration.

The evaluation of statistical uncertainty on each phase differences data extracted from fractional frequency differences, is given as we have in presence of white frequency noise in each period of measurement, by the expression

$$\sigma_x(\tau_i)^2 = \sigma_y(\tau_i)^2\ \tau_i^2$$

For the whole period T of measurement that gives in frequency instability

$$\sigma_y(\tau) = \frac{\sqrt{\sum_{i=1}^{N} \sigma_y(\tau_i)^2\ \tau_i^2}}{T}$$

With N =25, from 26th October to 20th November and $T = 86400\ MJD_{fin} - 86400\ MJD_{deb} = 0.2182888224\ 10^7$ seconds it gives

$$\sigma_y(\tau) = \frac{\sqrt{\sum_{i=1}^{25} \sigma_y(\tau_i)^2\ \tau_i^2}}{T} = 0.611\ 10^{-16}$$

$$\boxed{\sigma_A = 0.611\ 10^{-16}}$$

The evaluation of the mean frequency between two intervals of integrations during the period from MJD 53304 to MJD 53329 is given by equation (2) and calculated for frequency fluctuation difference measurements. Figure 14 shows the frequency differences between H_Maser 1400816 and FO2 (blue plus) and the mean frequency during dead times (magenta stars).

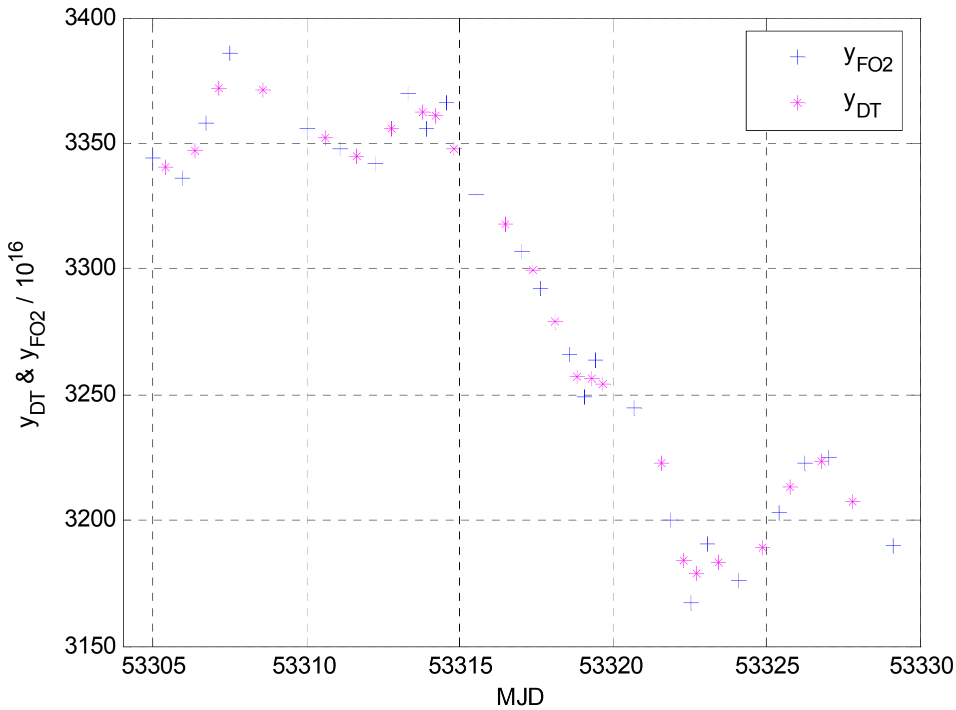

Figure 14: frequency differences H_Maser1400816 and FO2 from MJD 53304 up to MJD 53329

From equation (3) we find the phase difference over the whole period of integration

$$x_{fin} - x_{deb} = 0.71695119\ \mu s$$

This value is replaced in equation (4) above for computation of y_{moy} during this period. We find

$$\boxed{y_{moy} = 0.328441\ 10^{-12}}$$

ANNEXE 6

Mean Frequency between H Masers 1400805 and 1400816 computed by phase differences over MJD 53304 to 53329

On figure 15 is shown the evolution of the differences between phase differences $x_{[k]}$(H805)- $x_{[k]}$(H816) with a periodic measurement of 100s. From MJD_{deb} 53304.00078 up to MJD_{fin} 53329.99982 results N=22463 samples.

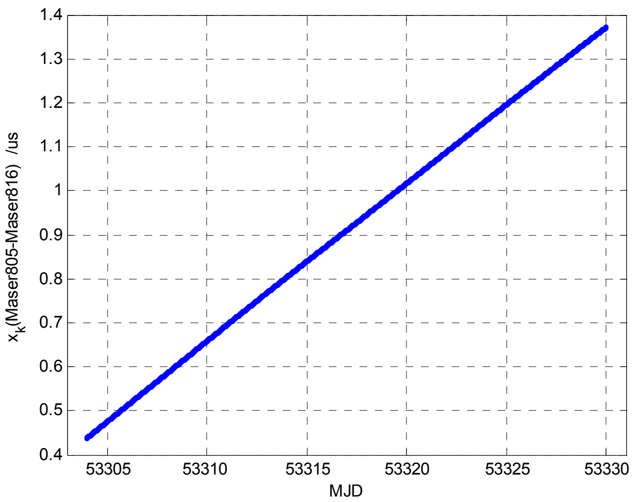

Figure 15: Phase differences Maser805-Maser816

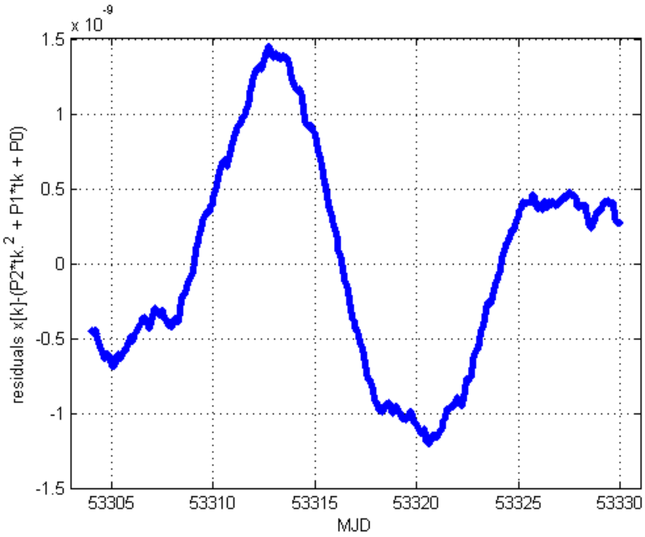

Figure 16: residuals of phase between Masers after quad fit removed

By using a second order polynomial fitting the phase differences data $x_{[k]}$(H805)- $x_{[k]}$(H816) : $x(t) := P_1\, t^2 + P_2\, t + P_3$

P1 = -3.07349162581701e-011; P2 = 3.31325721890051e-006; P3 = -0.0892818024297861 ;

The mean frequency with this polynomial fit order 2 over the phase differences is given by:

$$y_{moy} = \frac{1}{86400}\left(\frac{1}{MJD_{fin} - MJD_{deb}} \int_{MJD_{deb}}^{MJD_{fin}} 2\, P_1\, t + P_2\, dt\right)$$ which is equivalent to

$$y_{moy} = \left(\frac{1}{86400} MJD_{deb} + \frac{1}{86400} MJD_{fin}\right) P_1 + \frac{1}{86400} P_2$$

Figure 16 shows residuals obtained after this quadratic fit removed. The 2 *ns* pick to pick residuals results to a frequency instability over the 25 days of $9{,}25 \times 10^{-16}$.

➔ $(y_k)_{moy}$= 4.151,63x 10^{-16} ± 9,25 x 10^{-16}

Frequency difference between Masers obtained by phase difference between beginning and ending of the whole period gives ➔ **$(y_k)_{moy}$= 4.154,86 x 10^{-16}** with statistical uncertainty corresponding to $u_A(y_k)_{moy}=2\sigma_{meas}/T$ with σ_{meas} = 2ps of the time interval counter Stanford Research SR620 and T= 2246317s ➔ **$u(y_k)_{moy}$ = 1,8 x 10^{-18}**.

$$\boxed{y_{H805-H816} = 0.415486\ 10^{-12}} \qquad \boxed{u_A(y_{H805-H816}) = 0.18\ 10^{-17}}$$

Systematic error is evaluated with the time interval error of the time interval counter Stanford Research SR620:

Error < ± (500 ps typ. [1 ns max.] + Timebase Error ´ Interval + Trigger Error)

Considering the 3σ time interval error equal to 1 ns, the 1σ = 333,33ps. The evaluation of Time base Error is 1,35ps and the Trigger error is 0,23ps on input A and 0,23ps on input B of the counter. So we obtain $\sigma_{x(Counter)}(1\sigma)$ = 335 ps that is divided by a factor 100 corresponding to the phase difference multiplication used with the counter. From the frequency mean resulting from the first phase difference between the whole interval periods, the uncertainty is computed by

$\sigma_B(yk)_{moy} = 2\sigma_{x(Counter)}/T$ ➔ $\boxed{u_B(y_{H805-H816}) = 0.298\ 10^{-17}}$

This result can be verified in consistency with the daily measurements of phase differences between Masers and the atomic local time scale UTC(OP). The differences between the phase differences x_k(H805-UTC(OP)) and x_k(H816-UTC(OP)) is plotted on figure 17 from MJD 53304 and MJD 53329.

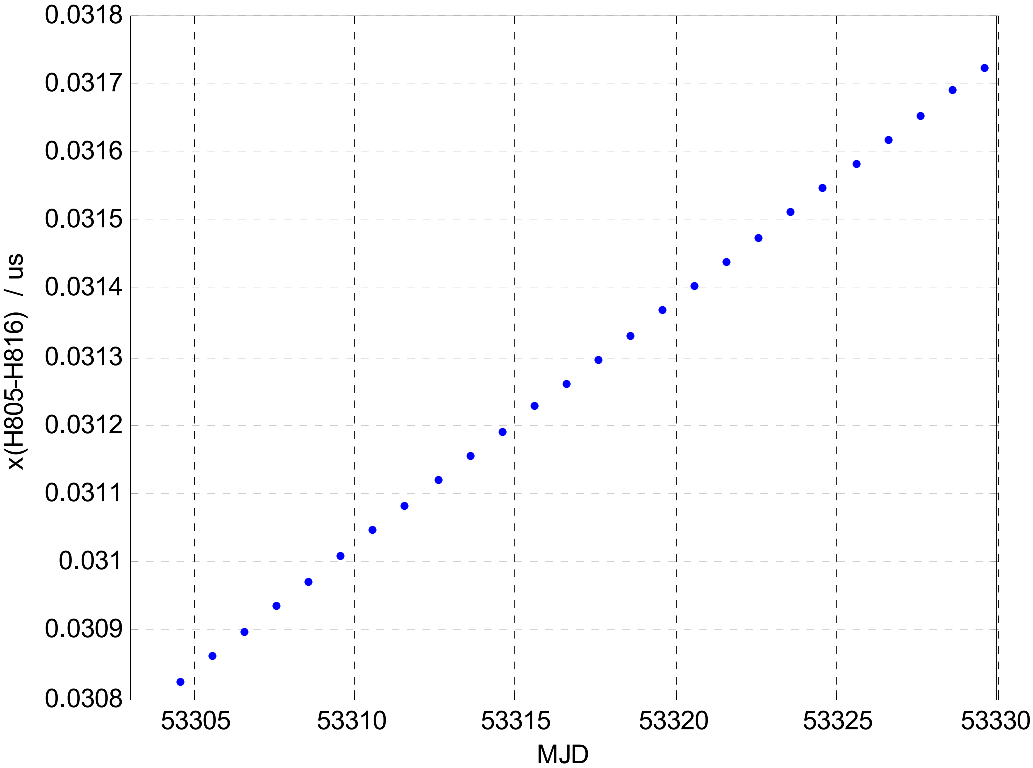

Figure 17: Phase differences (Maser805-UTC(OP)) – (Maser816 – UTC(OP))

Frequency difference between Masers obtained by phase difference between beginning and ending of the whole period gives ➔ $(y_k)_{moy}$= **4152,78 x 10^{-16}** with statistical uncertainty corresponding to u_x =sqrt(2).u_x(t) with u_x(t)=150ps ➔ u_x=212ps and over the 25 days of the whole period $u_y(y_{moy})$ = 0,98 x 10^{-16} . The mean frequency obtains by these daily phase difference measurements Maser-UTC(OP) is resumed by:

➔ $(y_k)_{moy}$= 4152,78 x 10^{-16} ± 0,98 x 10^{-16}

The frequency difference between these two frequency averages is 2 x 10^{-16} that is compatible with their respective uncertainties.

REFERENCES

[ref. 1] - C. Vian, P. Rosenbusch, H. Marion, S. Bize, L. Cacciapuoti, S. Zhang, M. Abgrall, D. Chambon, I. Maksimovic, P. Laurent, G. Santarelli, A. Clairon of Obs. Paris, SYRTE, A. Luiten, M. Tobar, Univ. W. of Australia School of Physics, C. Salomon of LKB, "BNM-SYRTE Fountains: Recent Results", to be published in **Proceedings CPEM 2004**.

[ref. 2] - F. Pereira Do Santos, H. Marion, M. Abgrall, S. Zhang, Y. Sortais, S. Bize, I. Maksimovic, D. Calonico, J. Grünert, C. Mandache, C. Vian, P. Rosenbusch, P. Lemonde, G. Santarelli, Ph. Laurent and A. Clairon of BNM-SYRTE, C. Salomon of LKB, "Rb and Cs Laser Cooled Clocks: Testing the Stability of Fundamental Constants". **Proceedings IEEE 2003, EFTF Tampa May 2003, p 55-67.**

[ref. 3] - P. Wolf of BNM SYRTE, C.J. Bordé of LPL, "Recoil effects in microwave Ramsey spectroscopy", arxiv: **quant-ph/0403194**.

[ref. 4] - F. Pereira Do Santos, H. Marion, S. Bize, Y. Sortais, A. Clairon, and C. Solomon "Controlling the Cold Collision Shift in High Precision Atomic Interferometry" of, **Phys, Rev, Lett, 89,233004 (2002)**.

[ref. 5] - J. Vanier, C. Audouin, « The Quantum Physics of Atomic Frequency Standards », **Adam Hilger, Bristol & Philadelphia (1989)**.

[ref. 6] - R. Schröder, U. Hübner and D. Griebsch, "Design and Realization of the Microwava Cavity in PTB Caesium Atomic Clock CSF1" **IEEE Trans. Instrum. Meas., vol. 49, p.383, 2002**.

[ref. 7] - L. Cutler *et al*, "Frequency pulling by hyperfine σ - transitions in cesium atomic frequency standards, **J. Appl. Phys. Vol. 69, pp. 2780, 1991**.

[ref. 8] - A. Bauch, R. Schröder "Frequency shift in Caesium Atomic Clock due to Majorana transitions", Annalen der Physik**, vol. 2, pp. 421, 1993**.

[ref. 9] – H. Marion thèse de doctorat de l'Université de Paris 6 (To be published)